

An alternative way to locally measure the Hubble constant using Gravitational Waves and Pulsar Timing Arrays

JORGE ALFARO¹ AND MAURICIO GAMONAL¹

¹*Instituto de Física*

*Pontificia Universidad Católica de Chile
Av. Vicuña Mackenna 4860, Santiago, Chile.*

(Received March 5, 2019)

Submitted to ApJ

ABSTRACT

Recent research show that the cosmological components of the Universe should influence on the propagation of Gravitational Waves (GWs). Moreover, it has been proposed a new way to measure the cosmological constant using Pulsar Timing Arrays (PTAs). However, these results have considered very particular cases (e.g. a de Sitter Universe or a mixing with non-relativistic matter). In this work we propose an extension of these results, using the Hubble constant as the natural parameter that includes all the cosmological information, studying its consequences on the propagation of GWs and exploring the possibilities of a local measurement. From linearized gravity we consider a mixture of perfect fluids permeating the spacetime and study the propagation of GWs within the context of the Λ CDM model. Using this framework we found a relationship, e.g. an analytical expression and an approximation that differs by 1.5% from numerical simulations, between the local value of the Hubble constant and some observables of Pulsar Timing Array experiments. The results show that the value of H_0 is relevant within the measurement of pulsars timing residual and the simulations show that, under the accuracy expected by the IPTA collaboration in the next years, this effect could be eventually observed.

Keywords: cosmology: theory — cosmological parameters — gravitational waves — pulsars: general

1. INTRODUCTION

In the last two decades a lot of astronomical evidence has been found that suggests our Universe is expanding at an accelerated rate (Perl-

mutter et al. 1997; Riess et al. 1998; Planck Collaboration et al. 2018; Riess et al. 2018). This observation is a cornerstone of modern cosmology and represents an ideal setting in which the large scale aspects of gravitation can be tested. In that sense, General Relativity provides a standard framework in which it is possible to model the cosmological observations:

Corresponding author: Jorge Alfaro
jalfaro@uc.cl, mfgamonal@uc.cl

The Λ CDM standard model of Cosmology (a full review can be found in [Bull et al. 2016](#)), which through the action of the unknown Dark Matter and Dark Energy, can precisely describe our flat, isotropic, homogeneous and expanding Universe.

Within the Λ CDM model, the variable that describes the rate of expansion is the *Hubble parameter* and its value at the present day, the **Hubble constant**, is denoted by H_0 . The value of H_0 represents the current rate of expansion and contains information of the Universe composition. Recently there has been great controversy about its actual value, in particular, from the tension in the data obtained using the CMB spectrum ([Planck Collaboration et al. 2018](#)) and the local observation of standard candles ([Riess et al. 2018](#)). This fact has generated new questions regarding the local behavior of H_0 and many possible explanations to the phenomenon have been raised: From possible new physics to as-yet unrecognized uncertainties from the observations ([Odderskov et al. 2014](#); [Ko & Tang 2016](#); [Freedman 2017](#); [Bringmann et al. 2018](#); [Camarena & Marra 2018](#); [Mörtsell & Dhawan 2018](#); [Di Valentino et al. 2018](#); [Feeney et al. 2019](#)). Nevertheless, no consensus has been reached so far and an intense debate is still going on, waiting for improved experimental data.

On the other hand, in recent years, the measurement of **Gravitational Waves** (GW) done by the ground-based detector, LIGO ([Abbott et al. 2016](#)), has revolutionized the scientific scenario and its use in cosmology was immediate: A gravitational-wave standard siren was used to measure the Hubble constant independently ([LIGO Collaboration et al. 2017](#)). This observation show us that the efforts involved in the accurate measurement of gravitational waves could be useful in the analysis of cosmological

parameters within the next years. Furthermore, another type of ongoing gravitational-wave experiment is the **Pulsar Timing Array** (PTA), which uses the residual time of the arriving electromagnetic emissions from different millisecond-pulsars located in the Milky Way (for a review of PTA research see [Hobbs & Dai 2017](#)) and their correlations to determine the presence of gravitational radiation. With that goal, the International Pulsar Timing Array collaboration (IPTA) is established ([Hobbs et al. 2010](#)) as a multi-institutional cooperation of diverse projects around the world, which together, seek to identify and measure low-frequency (i.e. $\sim 10^{-9}$ to 10^{-8} Hz) gravitational waves coming from astrophysical sources as supermassive binary black hole mergers or even a possible background of them (the first release of data from the IPTA collaboration can be found in [Verbiest et al. 2016](#)).

The theoretical work of [Bernabeu et al. \(2011\)](#) shows that, using a coordinate transformation between a Schwarzschild-de Sitter metric and the corresponding Friedmann-Lemaître-Robertson-Walker (FLRW) metric for a *de Sitter Universe*, the propagation of gravitational waves (e.g. its frequency and wave number) are affected by the cosmological constant Λ . Moreover, in [Espriu & Puigdomènech \(2013\)](#); [Espriu \(2014\)](#) was proposed that the magnitude of residual time in a PTA experiment could change due to the action of the cosmological constant. A complete explanation of this effect can be found in the work of [Alfaro et al. \(2019\)](#), where also was included the action of non-relativistic matter into the phenomenon, showing that Dark Matter increases the effect of Dark Energy on the propagation of gravitational waves.

The aim of this work is to show that, following the line of research developed in [Bernabeu et al.](#)

(2011); Espriu & Puigdomènech (2013); Espriu (2014); Alfaro et al. (2019), the propagation of Gravitational Waves is actually affected by all the cosmological components of the Universe valued at the present day, i.e. by the Hubble constant. In particular, this model allows us to find, by reasonable approximations, an explicit formula that relates an specific observable of a PTA experiment (i.e. the angle between the pulsar and the source of gravitational waves) involved in the timing residual of the light coming from pulsars and the value of the Hubble constant. We will show that this relationship could be possibly tested by future successful observations of the IPTA collaboration and, therefore, this framework could serve as a theoretical basis for an independently measurement of the Hubble constant using the analysis of Gravitational Waves from PTA experiments.

This paper is structured as follows: In subsection 2.1 we review the theoretical formalism of the linearized version of General Relativity and the standard Λ CDM model of cosmology, meanwhile in the subsection 2.2 we present the main ideas developed in the line of work previously mentioned and our findings when we use the Hubble constant as the parameter that governs the dynamics of the GW propagation. The entire section 3 is devoted to analyze the possibility of using PTA experiments to observe the studied phenomenon: In subsection 3.1 we shortly explain the working of PTA and in subsection 3.2 we show how our framework can be tested using the previous setup. Furthermore, in subsection 3.3 we present a reasonable approximation that give us a direct relationship between a PTA observable and the value of the Hubble constant. Finally, in section 4 we present our conclusions and an outlook for future research.

2. GRAVITATIONAL WAVES IN AN EXPANDING UNIVERSE

2.1. Linearized Theory of General Relativity and Standard Cosmology

The classical theory of General Relativity, finally consolidated in Einstein (1916), predicts that matter and the space-time curvature are related through the Field Equations,

$$G_{\mu\nu} + \Lambda g_{\mu\nu} = \kappa T_{\mu\nu}, \quad (1)$$

where $\kappa = 8\pi G/c^4$, $G_{\mu\nu}$ are the components of the Einstein tensor, $T_{\mu\nu}$ are the components of the stress-energy tensor and Λ is the cosmological constant, which plays an important role within the context of cosmology since it can be interpreted as the energy associated with vacuum and is commonly denoted as *Dark Energy*. The prediction of gravitational radiation (Einstein 1918), came from the linearization of (1) which is nothing else than doing perturbation theory around flat space-time, so the metric looks like

$$g_{\mu\nu} = \eta_{\mu\nu} + h_{\mu\nu}, \quad |h_{\mu\nu}| \ll 1. \quad (2)$$

The computation of the linearized Field Equations is usually obtained in any text of General Relativity (see Cheng 2010), giving

$$\square \bar{h}_{\mu\nu} = -2\Lambda \eta_{\mu\nu} - 2\kappa T_{\mu\nu}, \quad (3)$$

where $\bar{h}_{\mu\nu}$ is the trace-reversed perturbation defined by

$$\bar{h}_{\mu\nu} \equiv h_{\mu\nu} - \frac{1}{2}\eta_{\mu\nu}h, \quad (4)$$

which satisfies the Lorenz gauge condition

$$\partial_\beta \bar{h}^{\beta\alpha} = 0. \quad (5)$$

In Bernabeu et al. (2011); Espriu & Puigdomènech (2013); Alfaro et al. (2019) it is shown that the metric perturbation can be decomposed in different parts as $h_{\mu\nu} = h_{\mu\nu}^{(GW)} + h_{\mu\nu}^{(\Lambda)} + h_{\mu\nu}^{(bg)}$, which satisfy the following equations

$$\square \bar{h}_{\mu\nu}^{(GW)} = 0, \quad \square \bar{h}_{\mu\nu}^{(\Lambda)} = -2\Lambda \eta_{\mu\nu}, \quad \bar{h}_{\mu\nu}^{(bg)} = -2\kappa T_{\mu\nu}. \quad (6)$$

As explained there, the solution of $h_{\mu\nu}^{(\Lambda)}$ correspond to the linearization of a static spherically symmetric metric (i.e. the Schwarzschild-de Sitter metric) in the Lorenz gauge, through a time-independent and at order Λ coordinate transformation. As in this work the relevant corrections will be of order H_0 (i.e. $\sim \sqrt{\Lambda}$), the analysis of Gravitational Waves and the decomposition (6) will be simpler in the Lorenz gauge presented and as the perturbations from the Minkowski spacetime are very small when we are far away from the source, the linearization is justified. Thus, the contribution of different terms turns to be additive, what makes the discussion straightforward. If the source is located at a large (but non cosmological) distance, the perturbation will be described approximately by a combination of harmonic functions (Espriu 2014; Alfaro et al. 2019)

$$h_{\mu\nu}^{(\text{GW})} = \frac{\left(E_{\mu\nu} \cos[\Omega(t-r)] + D_{\mu\nu} \sin[\Omega(t-r)]\right)}{r} + \mathcal{O}(H_0^2), \quad (7)$$

where $E_{\mu\nu}$ and $D_{\mu\nu}$ are the components of the polarization tensors and Ω is the angular frequency of a *monochromatic* gravitational wave. It is important to note that the coordinates $\{t, r\}$ corresponds to a spherically symmetric context explained before and they will represent the frame which origin is placed at the –usually spherical shaped– source of Gravitational Waves.

On the other hand, in order to ensure the cosmological principle, the space-time can be described by the FLRW metric (for a complete review of standard cosmology see Cervantes-Cota & Smoot 2011)

$$ds^2 = -dT^2 + a^2(T) \left(\frac{dR^2}{1 - kR^2} + R^2 d\Omega^2 \right), \quad (8)$$

where $a(T)$ is the adimensional scale factor and in this metric the space-time is described by

comoving coordinates $\{T, R\}$. In this work we will use $k = 0$, which implies a globally flat geometry of the Universe, as it is currently observed (Planck Collaboration et al. 2018).

The stress-energy tensor that appears in (3) can be found by considering a perfect fluid (i.e. a fluid that has not viscosity and does not conduce heat), with energy density ρ and isotropic pressure p , filling the Universe. The components of $T^{\mu\nu}$ take the following form,

$$T^{\mu\nu} = (\rho + p)U^\mu U^\nu - pg^{\mu\nu}, \quad (9)$$

where U^μ are the components of the 4-velocity of the fluid. Inserting this expression into (3) we obtain the *Friedmann equations*: The first one from the 00-component and the second one from the trace,

$$\left(\frac{\dot{a}}{a}\right)^2 = \frac{\kappa}{3}(\rho_i + \rho_\Lambda) \equiv H^2(T) \quad (10)$$

$$\left(\frac{\ddot{a}}{a}\right) = \kappa \left(\frac{\rho_\Lambda}{3} - \frac{\rho_i}{6} - \frac{p_i}{2} \right), \quad (11)$$

where ρ_i and p_i are the energy density and the isotropic pressure of the i -th fluid respectively and $H(T)$ is the *Hubble parameter*, which value at the present day, i.e. $H(T_0) \equiv H_0$, is known as the **Hubble constant** H_0 . In order to obtain the time evolution of the scale factor an equation of state must be provided. In Alfaro et al. (2019) was used $p = 0$, which corresponds to the equation of state of non-relativistic dust. However, in this work we will use $p_i = \omega_i \rho_i$, with ω_i constant, in order to develop a general discussion of the phenomenon. Using the Friedmann equations we can find that

$$\frac{\rho_i}{\rho_0} = \left(\frac{a(T)}{a_0} \right)^{-3(\omega_i+1)}, \quad (12)$$

where $\rho_0 = \rho(T_0)$ is the current energy density of the i -th fluid and $a_0 = a(T_0)$ is the current scale factor (usually taken as 1), and both are

integration constants. Replacing this expression into (10) provides a solution of the scale factor in terms of the comoving time and the equation of state,

$$a(T) = \begin{cases} a_0 \left(\frac{T}{T_0} \right)^{\frac{2}{3(\omega_i+1)}} & \text{if } \omega_i \neq -1 \\ a_0 \exp\left(\sqrt{\frac{\Lambda}{3}}(T - T_0)\right) & \text{if } \omega_i = -1 \end{cases}. \quad (13)$$

In the $\omega_i \neq -1$ case, when we combine (12) with (13) we can obtain the general form of the energy density of the i -th fluid,

$$\rho_i = \begin{cases} \frac{4}{3(\omega_i + 1)^2 \kappa T^2} & \text{if } \omega_i \neq -1 \\ \Lambda/\kappa & \text{if } \omega_i = -1 \end{cases}. \quad (14)$$

Currently, the standard cosmological model is the Λ CDM: Includes a positive cosmological constant Λ (which represents the so-called Dark Energy) and Cold Dark Matter (which is the union of baryonic matter and non-relativistic dark matter). In the Λ CDM model, when a global flat geometry is considered, we can use (12) to write an effective energy density in terms of the scale factor and the currently evaluated energy densities,

$$\begin{aligned} \rho_{\text{eff}} &= \rho_\Lambda + \rho_d + \rho_r \\ &= \rho_\Lambda + \rho_{d0} \left[\frac{a_0}{a(T)} \right]^3 + \rho_{r0} \left[\frac{a_0}{a(T)} \right]^4, \end{aligned} \quad (15)$$

where $\rho_\Lambda = \Lambda/\kappa$, ρ_{d0} is the current density of non-relativistic matter (i.e. Cold Dark Matter and baryonic matter, $\omega_d = 0$) and ρ_{r0} is the current radiation density ($\omega_r = 1/3$).

These expressions will be used in the next sections in order to construct a spherically symmetric metric which reproduces the corresponding spacetime geometry of a FLRW metric for a perfect fluid with an arbitrary ω_i .

2.2. Coordinate transformation and an application to the Λ CDM model

Let us consider the following situation: Two remote galaxies are merging so their central super-massive black holes are orbiting around a common center of mass and slowly approaching to each other. This is basically a Keplerian problem with \sim approximate \sim spherical symmetry. For this reason, near the source of gravitational waves, a spherically symmetric set of coordinates, i.e. $\{t, r, \theta, \phi\}$, is very useful in order to describe space-time and their perturbations. A very detailed discussion about these considerations are given in [Espriu \(2014\)](#), where also is established that Gravitational Waves in their simplest form and expressed in these source-centered coordinates will have the form given in the equation (7).

However, these coordinates are not useful in cosmology because the cosmological measurements are described in comoving coordinates, i.e. $\{T, R, \theta, \phi\}$. Thus, the main objective of this line of work is to find the coordinate transformation between the GW-source-centered and the comoving coordinates. For a compendium with all the results found before the writing of this paper, including the coordinate transformations of a de Sitter Universe in FLRW space-time and the Schwarzschild-de Sitter metric and the case where non-relativistic matter is added, besides other implications, see [Alfaro et al. \(2019\)](#).

The easiest example that we can give to illustrate what we have said before is showing the de Sitter case, where only the action of the cosmological constant is taken account. We note that in a vacuum background, an approximately spherical source of GW would produce a Schwarzschild metric. Thus, if we take $\Lambda \neq 0$, then when we are far from the source (i.e. neglecting the mass term), the geometry of space-

time will be described by the Schwarzschild-de Sitter (SdS) metric

$$ds^2 = - \left(1 - \frac{\Lambda}{3} r^2 \right) dt^2 + \frac{dr^2}{1 - \frac{\Lambda}{3} r^2} + r^2 d\Omega^2. \quad (16)$$

On the other hand, the FLRW metric – expressed in comoving coordinates – will be given by (8) and the scale factor is of the form (13) when $\omega_i = -1$. The main idea is to express the coordinates of the SdS metric in terms of the comoving coordinates of the FLRW metric, as they are two equivalent representations of the same spacetime. Using the second rank tensor property of the metric tensor when we perform coordinate transformations,

$$g_{\mu'\nu'} = \frac{\partial X^\mu}{\partial x^{\mu'}} \frac{\partial X^\nu}{\partial x^{\nu'}} g_{\mu\nu}, \quad (17)$$

one can arrive to the following transformations

$$r(T, R) = a(T)R \quad (18)$$

$$t(T, R) = T - \sqrt{\frac{\Lambda}{3}} \ln \sqrt{1 - \frac{\Lambda}{3} a(T)^2 R^2}. \quad (19)$$

An expansion at order $\sqrt{\Lambda}$ of these transformations gives us

$$r(T, R) = a_0 R \left[1 + \Delta T \sqrt{\frac{\Lambda}{3}} \right] + \mathcal{O}(\Lambda) \quad (20)$$

$$t(T, R) = T + a_0^2 \left(\frac{R^2}{2} \sqrt{\frac{\Lambda}{3}} \right) + \mathcal{O}(\Lambda). \quad (21)$$

This is the result shown in [Bernabeu et al. \(2011\)](#); [Espriu & Puigdomènech \(2013\)](#), which was the starting point of this line of work. From these transformations was found how affects the cosmological constant on the propagation of gravitational waves and in [Espriu \(2014\)](#) was explained how this effect could be measured using Pulsar Timing Arrays. These expressions show us how comoving coordinates (and their corresponding cosmological parameters) are related

to the coordinates in the SdS metric, whereby when replacing in (7) it would show how GW are seen by a cosmological observer, that is the main idea and it is what we are going to exploit next.

In order to develop a more general discussion of the phenomenon, we will consider in first place a Universe filled by a single fluid with an arbitrary equation of state, i.e. $p_i = \omega_i \rho_i$. The methodology to be used is basically build a diagonal, spherically symmetric and asymptotically flat metric (that we will denote by $SS\omega_i$), described in the coordinates $\{t, r\}$, that recovers the corresponding FLRW metric in comoving coordinates, then find the coordinate transformation between both frames and, finally, replace the coordinates in (7), showing how it affects on the propagation of gravitational radiation.

As we have to impose a spherically symmetric geometry we will have the transformation $r^2 d\Omega^2 \rightarrow a(T)^2 R^2 d\Omega^2$. Using the metric tensor property (17) and the requirement that the new metric must be diagonal, we obtain the relation

$$0 = \frac{\partial T}{\partial t} \frac{\partial T}{\partial r} g_{TT} + \frac{\partial R}{\partial t} \frac{\partial R}{\partial r} g_{RR}. \quad (22)$$

Computing the partial derivatives gives us the expressions

$$\frac{\partial R}{\partial r} = -\frac{1}{3} \frac{2r \frac{\partial T}{\partial r} - 3T(\omega_i + 1)}{a(T)(\omega_i + 1)T} \quad (23)$$

$$\frac{\partial R}{\partial t} = -\frac{2}{3} \frac{r \frac{\partial T}{\partial t}}{a(T)(\omega_i + 1)T}, \quad (24)$$

and from (22) we find that

$$\frac{\partial T}{\partial r} = \frac{a(T)^2}{\frac{\partial T}{\partial t}} \frac{\partial R}{\partial t} \frac{\partial R}{\partial r}. \quad (25)$$

Thus, from the last equation, $\frac{\partial T}{\partial r}$ becomes

$$\frac{\partial T}{\partial r} = \frac{6rT(\omega_i + 1)}{4r^2 - 9(\omega_i + 1)^2 T^2}, \quad (26)$$

and using (17) we can obtain the components of the metric,

$$g_{tt} = -\left(\frac{\partial T}{\partial t}\right)^2 \left[\frac{9(\omega_i + 1)^2 T^2 - 4r^2}{9(\omega_i + 1)^2 T^2} \right] \quad (27)$$

$$g_{rr} = \frac{9(\omega_i + 1)^2 T^2}{9(\omega_i + 1)^2 T^2 - 4r^2}. \quad (28)$$

From (12) we can write the $SS\omega_i$ metric as

$$ds^2 = -\frac{(\partial_t \rho_i)^2}{3\kappa \rho_i^3 (\omega_i + 1)^2} \left[1 - \frac{\kappa \rho_i r^2}{3} \right] dt^2 + \frac{dr^2}{1 - \frac{\kappa \rho_i r^2}{3}} + r^2 d\Omega^2, \quad (29)$$

but, using (12) and (26), we get

$$\frac{\partial \rho_i}{\partial r} = \frac{(\omega_i + 1)\kappa \rho_i^2 r}{1 - \frac{\kappa \rho_i r^2}{3}}. \quad (30)$$

If we properly redefine $\tilde{\rho}_i \equiv \kappa \rho_i$, the last expression becomes

$$\frac{\partial \tilde{\rho}_i}{\partial r} = \frac{(\omega_i + 1)\tilde{\rho}_i^2 r}{1 - \frac{\tilde{\rho}_i r^2}{3}}, \quad (31)$$

but it can be noticed from (31) we can form the expression

$$\frac{\partial}{\partial r} \left[\frac{c + r^2 \tilde{\rho}_i}{\tilde{\rho}_i^n} \right] = 0, \quad (32)$$

where c and n are unknown constants that we suppose exist. Unfolding the last expression and using the linear independence of r , we obtain that the constants are

$$c = \frac{6}{3\omega_i + 1} \quad n = \frac{3\omega_i + 1}{3(\omega_i + 1)}. \quad (33)$$

Therefore, we can integrate (32) and write

$$\frac{c + r^2 \tilde{\rho}_i}{\tilde{\rho}_i^n} = F(t), \quad (34)$$

where $F(t)$ is a function only with respect to r . By a dimensional analysis, we note that in natural units $[\tilde{\rho}_i] = L^{-2}$ and therefore $[F(t)] = L^{2n}$.

As there is no other parameter involved apart from t , and also as $[t] = L$ in natural units, then we set $F(t) = At^{2n}$, with A as a dimensionless arbitrary constant. For any fluid we can expect that at later stage it will be diluted homogeneously, which implies that for $t \rightarrow \infty$ the metric (29) is almost flat. Then,

$$\lim_{t \rightarrow \infty (\rho_i \rightarrow 0)} \frac{(\partial_t \rho_i)^2}{3\kappa \rho_i^3 (\omega_i + 1)^2} = 1. \quad (35)$$

On the other hand, (34) can be written as

$$\frac{c + r^2 \kappa \rho_i}{(\kappa \rho_i)^n} = At^{2n}, \quad (36)$$

but when we take the derivative with respect to t and solving for $\partial_t \rho_i$, we obtain

$$\frac{\partial \rho_i}{\partial t} = -\frac{2nAt^{2n-1}(\kappa \rho_i)^n \rho_i}{\kappa \rho_i n r^2 - r^2 \kappa \rho_i + cn}, \quad (37)$$

and if we square, divide by $3\kappa \rho_i^3$ and replace the previous results, we can found the following equality

$$\frac{(\partial_t \rho_i)^2}{3\kappa \rho_i^3 (\omega_i + 1)^2} = \frac{4n^2 A^{1/n} (\kappa r^2 \rho_i + c)^{\frac{2n-1}{n}}}{3(\omega_i + 1)^2 [(n-1)\kappa r^2 \rho_i + cn]}. \quad (38)$$

Computing the limit $\rho_i \rightarrow 0$ as the fluid dilutes in very distant times, we can set the value of A ,

$$\lim_{t \rightarrow \infty (\rho_i \rightarrow 0)} \frac{(\partial_t \rho_i)^2}{3\kappa \rho_i^3 (\omega_i + 1)^2} = \frac{4n^2 A^{1/n} c^{\frac{2n-1}{n}}}{3(\omega_i + 1)^2 (cn)^2}, \quad (39)$$

and using that the metric is asymptotically flat, which implies that the previous limit is equal to one, we get the value of A ,

$$A = c \left(\frac{3}{4} \right)^n (\omega_i + 1)^{2n}. \quad (40)$$

Finally, with the constant A known, we can provide an exact expression for the the $SS\omega_i$ metric, which becomes

$$ds^2 = - \frac{dt^2}{\left(1 - \frac{\kappa\rho_i r^2}{3}\right) \left(1 + \frac{\kappa\rho_i r^2(3\omega_i + 1)}{6}\right)^{\frac{1-3\omega_i}{1+3\omega_i}}} + \frac{dr^2}{1 - \frac{\kappa\rho_i r^2}{3}} + r^2 d\Omega^2, \quad (41)$$

and from (36) we can express the coordinate transformation between the SS ω_i and the FLRW frames in terms of ρ_i y ρ_0 ,

$$t = \frac{\left[c + R^2(\kappa\rho_0)^{\frac{2}{3(\omega_i+1)}}(\kappa\rho_i)^{\frac{3\omega_i+1}{3(\omega_i+1)}}\right]^{\frac{1}{2n}}}{\left(A^{\frac{1}{2n}}\right) \sqrt{\kappa\rho_i}} \quad (42)$$

$$r = R \left(\frac{\rho_0}{\rho_i}\right)^{\frac{1}{3(\omega_i+1)}}. \quad (43)$$

The expansion of (42) and (43) in terms of the the energy density of the fluid at the present day, i.e. ρ_0 , becomes

$$t = T + \frac{R^2}{2} \sqrt{\frac{\kappa\rho_0}{3}} + \frac{R^2}{12} (1 - 3\omega_i) \kappa\rho_0 \Delta T + \mathcal{O}(\kappa^2 \rho_0^2) \quad (44)$$

$$r = R \left(1 + \Delta T \sqrt{\frac{\kappa\rho_0}{3}} - \frac{\kappa\rho_0 \Delta T^2}{12} (1 + 3\omega_i)\right) + \mathcal{O}(\kappa^2 \rho_0^2). \quad (45)$$

These results agree with what was found in Espriu (2014); Alfaro et al. (2019) and show that no matter the equation of state of the fluid, the lower order of expansion is always at order $\sqrt{\rho_0}$. Using this fact, we can expand the First Friedmann equation (10) at first order in H_0 , which contains the present day composition of the Universe, giving an expression for the scale factor,

$$a(T) = 1 + H_0 \Delta T + \mathcal{O}(H_0^2), \quad (46)$$

where H_0 is the *Hubble constant*, which is of the form

$$H_0 = \sqrt{\frac{\Lambda}{3} + \frac{\kappa\rho_{d0}}{3} + \frac{\kappa\rho_{r0}}{3}}. \quad (47)$$

As the r coordinate have to transform as $r \rightarrow a(T)R$ in order to preserve spherical symmetry, a comparison between (44), (45) and (46) shows that the cosmological components are added inside the square root, as was discussed in Alfaro et al. (2019) in the case of non-relativistic matter. Thus, in order to obtain the correct limits in all the previous models, the most general linearized coordinate transformations must be of the form

$$t = T + \frac{R^2}{2} H_0 + \mathcal{O}(H_0^2) \quad (48)$$

$$r = R(1 + \Delta T H_0) + \mathcal{O}(H_0^2). \quad (49)$$

Note that these are linear in H_0 , so only small effects will be considered. When replacing (48) and (49) into (7), we get

$$h'_{\mu\nu}^{(\text{GW})} = \frac{(1 - RH_0)}{R} (E'_{\mu\nu} \cos[w_{\text{eff}}T - k_{\text{eff}}R] + D'_{\mu\nu} \sin[w_{\text{eff}}T - k_{\text{eff}}R]), \quad (50)$$

where the new angular frequency (showing the expected redshift) and the new wave number are given by

$$w_{\text{eff}} \equiv \Omega(1 - RH_0) \quad k_{\text{eff}} \equiv \Omega\left(1 - \frac{R}{2}H_0\right). \quad (51)$$

In the last two expressions we can infer how the Hubble constant (i.e. all the cosmological parameters that describe the content of the Universe) affects the propagation of Gravitational Waves when a cosmological observer (e.g. laboratories in the surface of the Earth or local celestial bodies as pulsars) is measuring them, using comoving coordinates.

3. USING PTA TO MEASURE THE HUBBLE CONSTANT

3.1. Timing residual and the working of PTA

The results obtained in the last section, e.g. equations (50) and (51), show that the Hubble constant should influence in the propagation of Gravitational Waves. Now we will set an experimental framework in which this effect can be eventually measured. For this, we will use the light coming from a local pulsar and the shift in the arrival time of the pulse due to a gravitational radiation. In the following picture we show the simplest configuration, which will guide our discussion.

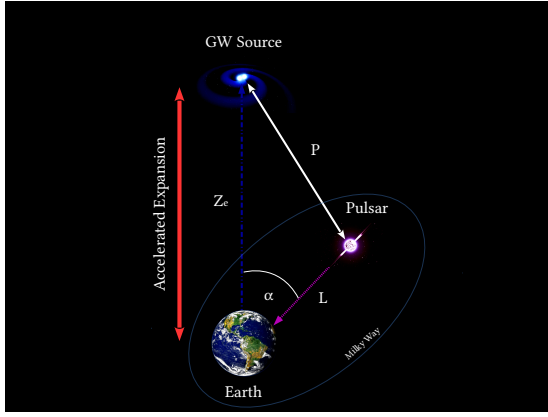


Figure 1. Setup of the configuration of our study: A source of gravitational waves ($R = 0$), the Earth ($Z = Z_e$) and a nearby Pulsar located at $\mathbf{P} = (P_X, P_Y, P_Z)$ referred to the source. The Z direction is chosen to be defined by the source-Earth axis. Polar and azimuthal angles are α and β respectively, from Z axis (self-elaborated image).

From Fig. 1, we note that the Earth and the pulsar are gravitationally bounded to the Milky Way, so they do not feel Universe expansion. However, the source of gravitational waves and the system Earth-pulsar are not bounded, so they do feel accelerated expansion and, therefore, the discussion and the result of previous chapter applies. The pulsar emits light with a particular electromagnetic field. Denoting the time-dependent phase of this field at the pul-

sar as ϕ_0 , then the phase of the electromagnetic pulse measured from Earth can be expressed as

$$\phi(T) = \phi_0 \left[T - \frac{L}{c} - \tau_0(T) - \tau_{\text{GW}}(T) \right] \quad (52)$$

where c the speed of light, $\tau_0(T)$ is the timing correction associated to the spacial motion of the Earth respect to the Solar system and $\tau_{\text{GW}}(T)$ is the timing correction due to the action of gravitational radiation incising in the system.

The correction due to the action of Gravitational Waves is given (Finn 2009; Deng & Finn 2011; Espriu 2014) by

$$\tau_{\text{GW}}(T) = -\frac{1}{2} \hat{n}^i \hat{n}^j H_{ij}(T), \quad (53)$$

where $\hat{n} = (-\sin \alpha \cos \beta, -\sin \alpha \sin \beta, \cos \alpha)$ is a unit vector pointing from Earth to the pulsar and H_{ij} is the integral of the metric perturbation along the null geodesic in the path pulsar-Earth, which could be parameterized by $\mathbf{R}(x) = \mathbf{P} + L(1+x)\hat{n}$ with $x \in [-1, 0]$. Using this path, $H_{ij}(T)$ takes the following form

$$H_{ij}(T) = \frac{L}{c} \int_{-1}^0 h'_{\mu\nu}^{(\text{GW})} \left(T + \frac{L}{c}x, |\mathbf{R}(x)| \right) dx. \quad (54)$$

3.2. Including the Λ CDM model and numerical analysis

In our framework (see Fig.1), the source of gravitational waves is far away from Earth, but not so the pulsar. Therefore, we can reasonable consider $L/Z_e \ll 1$ and then we can show that $\mathbf{R}(x) \approx Z_e + xL \cos \alpha$. Now we compute the equation (53) using (54). However, in the TT-Lorenz gauge, for a GW propagating through the Z axis, the only non-zero values of $E'_{\mu\nu}$ and $D'_{\mu\nu}$ are in the X,Y components (Bernabeu et al. 2011). We can also additionally assume, just for

simplicity, that $|E'_{\mu\nu}| = |D'_{\mu\nu}| \equiv \varepsilon \forall \mu, \nu$. Thus, the full timing residual in the arrival time of the

pulsar due to the pass of gravitational waves in the Λ CDM model becomes

$$\begin{aligned} \tau_{\text{GW}}^{\Lambda\text{CDM}} = & -\frac{L\varepsilon}{2c}(\sin^2 \alpha \cos^2 \beta + 2 \sin^2 \alpha \cos \beta \sin \beta - \sin^2 \alpha \sin^2 \beta) \\ & \times \int_{-1}^0 \frac{1 + H_0 [T_e + \frac{xL}{c}]}{Z_e + xL \cos \alpha} [\cos \Theta(x, \alpha) + \sin \Theta(x, \alpha)] dx, \end{aligned} \quad (55)$$

where

$$\Theta(x, \alpha) = \Omega \left(1 - \frac{Z_e + xL \cos \alpha}{c} H_0 \right) \left(T_e + \frac{xL}{c} \right) - \Omega \left(1 - \frac{Z_e + xL \cos \alpha}{2c} H_0 \right) \left(\frac{Z_e + xL \cos \alpha}{c} \right). \quad (56)$$

From a geometric argument, we can always fix the pulsar, the Earth and the source of gravitational waves in the same plane, thus we can set $\beta = 0$, and the independent parameter of τ_{GW} is the angle between the pulsar and the GW source measured from the Earth, α . In order to perform a numerical analysis we have to choose some reasonable values of the parameters that appear in the equation (55) and fix them to better visualize the behavior of the timing residual τ_{GW} . Thus, the setup described in the Fig. 1 can be modeled with the values that we show in the Table 1.

For the source of gravitational waves, we choose a typical distance Z_e where supermassive black holes are present and although is large, it is not a cosmological distance near to Big Bang. Otherwise, the distance between Earth and the pulsar is within the margin of a local galactic scale. It can be seen that $L \ll Z_e$, as required from the previous considerations. The angular frequency is of the expected order for future PTA projects and the same argument is used to fix ε , due to that it satisfies $|h| \sim \frac{\varepsilon}{R} \sim 10^{-15}$, where $|h|$ and Ω are within the expected accuracy of PTA projects, e.g. the EPTA (Babak et al. 2016) or the NANOGrav collaboration

Table 1. Simulation values

Parameter	SI value
Z_e	$3 \times 10^{24} \text{ m} \quad \sim 100 \text{ Mpc}$
T_e	$Z_e/c = 10^{16} \text{ s} \quad \sim 300 \text{ Myr}$
L	$10^{19} \text{ m} \quad \sim 1000 \text{ ly}$
Ω	10^{-8} rad/s
ε	$1.2 \times 10^9 \text{ m}$

NOTE—List of values considered for the parameters in the numerical integration of the timing residual τ_{GW} in (55), according to current accuracy of PTAs.

(Arzoumanian et al. 2018). Employing these parameters, the numerical integration of τ_{GW} value gives Fig. 2. As we can see, the value of the timing residual can be positive or negative. Since the meaningful physical magnitude is the amount of time, rather than the characteristic sign, we can also plot the absolute value of τ_{GW} , but now changing the value of the Hubble constant within a region of parameters, obtaining the Figure 3.

The most important feature of these figures is the presence of a considerable peak in the

value of the timing residual for a certain angle α . Moreover, we note that this peak changes its angular position with the value of the Hubble constant. This is our first clue of the existence of a distinguishable signal coming from the cosmological effects on the propagation of Gravitational Waves.

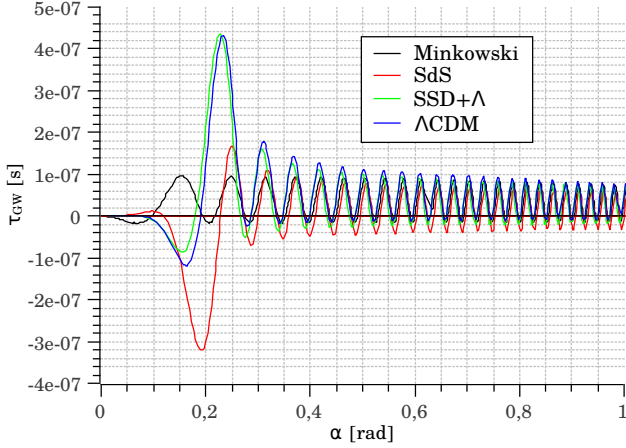


Figure 2. Comparison between different contents within the Universe. SdS is the only- Λ case, SDS+ Λ is where Dark Energy and Dark Matter (dust+ Λ) are taken account. The Λ CDM case also includes radiation. Note that in the Minkowski spacetime no peak is observed. This graphic also agrees with the results obtained in Alfaro et al. (2019).

In order to make an analysis of the possible signal shown in the previous figures, we will use some pulsars from the ATNF catalog Manchester et al. (2005). As we know, pulsars are stable clocks whose periods are known with great accuracy. Assuming a modest precision of $\sigma_t = 9.6 \times 10^{-7} s \approx 10^{-6} s$ which is obtained by averaging the precision achieved of best pulsars in the IPTA collaboration (Espriu 2014), we can define a *statistical significance* of the timing residual, of the form

$$\sigma = \sqrt{\frac{1}{N_p N_t} \sum_{i,j=1}^{N_p, N_t} \left(\frac{\tau_{GW}}{\sigma_t} \right)^2}, \quad (57)$$

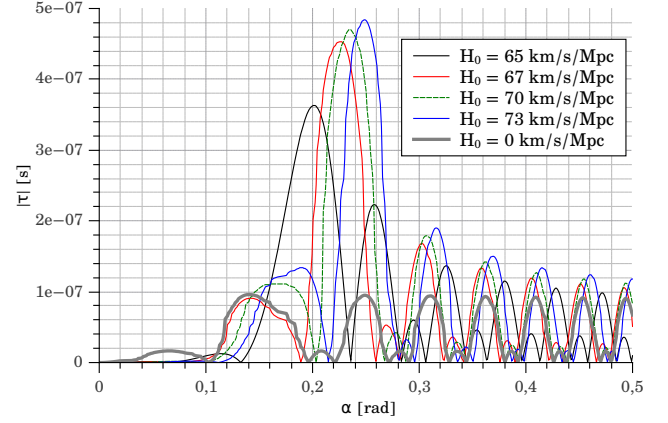


Figure 3. Numerical analysis of the absolute value of timing residual in terms of α , varying the value of the H_0 . We can note a characteristic peak at certain angle α_m , which increases with H_0 and how that peak slightly increases its angular position as we increase the value of H_0 .

where index i running from 1 to N_p (number of pulsars averaged) and j running from 1 to N_t (number of observations). Assuming we perform measurements every 11 days through 3 years, then $N_t = 101$. The pulsars belong to the considered cluster are shown in Table 2.

We will keep α as a free parameter and suppose that an hypothetical GW source is located at α radians between Earth and pulsars. Thus, the statistical significance is given by the following expression

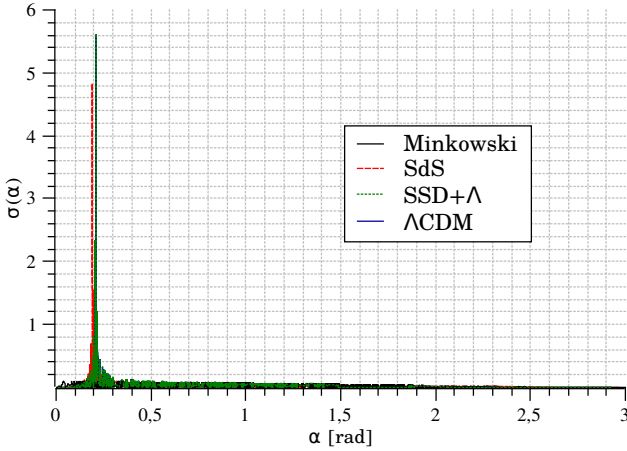
$$\sigma(\alpha) = \sqrt{\frac{1}{5 \cdot 101} \sum_{i=1}^5 \sum_{j=1}^{101} \left(\frac{\tau_{GW}(\beta_i)}{\sigma_t} \right)^2} \quad (58)$$

The result of the simulation can be observed in the Figure 4, showing the characteristic peak as we expected. However, we can develop a more realistic simulation. In the figure 4, only a cluster of 5 pulsars were considered and all of them were averaged at the same angle α . However, one can expect that all the pulsars are located at different angles (in galactic coordinates) and basically being randomly located. Therefore, we have considered 11 randomly distributed groups

Table 2. Pulsars from ATNF Catalog

Pulsar Name	ϕ	L_i
J0024-7204E	-44.89°	4.69 kpc
J0024-7204D	-44.88°	4.69 kpc
J0024-7204M	-44.89°	4.69 kpc
J0024-7204G	-44.89°	4.69 kpc
J0024-7204I	-44.88°	4.69 kpc

NOTE—List of pulsars averaged for an hypothetical source at angular separation α . It is shown the data given in [Manchester et al. \(2005\)](#), where ϕ is the galactic latitude—transformed to β_i — and L_i the distance between Earth and pulsar. We can note that this set simplify the computation of σ because all pulsars are very close to each other.

**Figure 4.** Simplified simulation of σ in an hypothetical observation of the peak in τ_{GW} . A huge peak is observed near 0.2 rad. Green and blue curves overlap due to the similarity of SSD+ Λ and Λ CDM models.

of 5 pulsars each (see Tab. 3), two test clusters of pulsars with a suitable location (65 pulsars in total) and a source of gravitational waves located at galactic coordinates $\theta_S = 20^\circ$ and

$\phi_S = 15^\circ$. Then, we averaged them using the statistical significance given by

$$\sigma_k = \sqrt{\frac{1}{5 \cdot 101} \sum_{i=1}^{5_k} \sum_{j=1}^{101} \left(\frac{\tau_{\text{GW}}(L_i, \alpha_i, \beta_i)}{10^{-6}} \right)^2} \quad (59)$$

and plot it as a function of the average angle of the group, namely $\bar{\sigma}_k = \sum_{i=1}^{5_k} \alpha_i / 5$. From this simulation we obtained Fig. 5, where we can note how the randomly distributed pulsars mostly do not show any signal, except for those that are located very close to the maximal angle, namely α_m , where the value of the timing residual is maximized. For a pulsar located within the vicinity of the angle α_m , the effect of the Hubble constant on the propagation of Gravitational Waves and the ability of measure them using a Pulsar Timing Array is extraordinarily increased.

This fact indicates that only the pulsars placed near the specific angle α_m with respect to the source of Gravitational Waves will show the characteristic peak in the timing residual with great statistical significance, which obviously implies a major obstacle when trying to observe this effect. Nevertheless, as more pulsars are observed and studied, it is more likely to measure with great certainty the existence of this peak, which could represent a challenge for the future astrophysical research of PTA experiments.

Table 3. Sets of pulsars from ATNF

Pulsar Name	θ	ϕ	L_i
J0324+5239	168.5°	-31.68°	2.56 kpc
J0325+67	145°	-1.22°	1.51 kpc
J0329+1654	130.31°	18.68°	1.05 kpc
J0332+5434	150.35°	-8.64°	1.54 kpc
J0332+79	169.99°	-30.04°	1.30 kpc

Table 3 continued

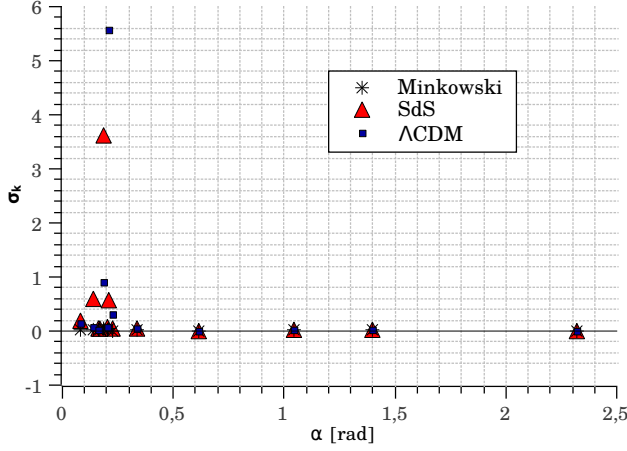


Figure 5. Numerical simulation of the statistical significance in the measurement of residual for three different models of the Universe. We used 13 sets with 5 pulsars each. For 11 of the sets, we took randomly distributed pulsars from the ATNF catalog (see Tab. 3), and 2 of them were test groups with suitable parameters, as the pulsars shown in Tab. 2. The larger peaks shown come from the test groups, showing the difficulty of doing actual successful measurements. Again, SdS is for a de Sitter Universe and Λ CDM for the full cosmological model. Note that if we consider only the Minkowski spacetime, no peak is observed.

Table 3 (*continued*)

Pulsar Name	θ	ϕ	L_i
J2007+2722	78.23°	2.09°	2.15 kpc
J2007+3120	68.86°	−4.67°	2.10 kpc
J2008+2513	76.89°	0.96°	10.3 kpc
J2009+3326	87.86°	8.38°	1.83 kpc
J2010-1323	86.86°	7.54°	2.06 kpc
J1848-1150	35.26°	1.4°	12.3 kpc
J1848+12	36.72°	2.23°	8.23 kpc
J1848-1243	44.99°	6.34°	2.17 kpc
J1848-1414	46.69°	7.29°	1.22 kpc
J1848-1952	32.54°	−0.33°	5.45 kpc
J1826-1256	21.33°	0.26°	4.94 kpc
J1826-1334	14.6°	−3.42°	5.94 kpc

Table 3 continued

Table 3 (*continued*)

Pulsar Name	θ	ϕ	L_i
J1826-1419	53.34°	15.61°	0.91 kpc
J1826-1526	29.76°	4.25°	10.3 kpc
J1827-0750	29.16°	3.99°	3.50 kpc
J1946+14	66.86°	2.55°	7.47 kpc
J1946+1805	44.86°	−10.55°	3.94 kpc
J1946+2052	61.1°	−1.17°	7.27 kpc
J1946+2244	50°	−7.74°	1.51 kpc
J1946+24	52.5°	−6.58°	1.59 kpc
J1946+24	30.81°	3.73°	3.35 kpc
J1831-1329	30.57°	3.45°	4.68 kpc
J1831-1423	27.04°	1.75°	2.49 kpc
J1832+0029	25.64°	0.96°	6.30 kpc
J1832-0644	25.17°	0.76°	8.29 kpc
J2155-3118	108.64°	6.85°	1.88 kpc
J2155-5641	89.66°	−22.81°	2.82 kpc
J2156+2618	87.69°	−26.28°	1.80 kpc
J2157+4017	106.65°	2.95°	3.00 kpc
J2203+50	107.15°	3.64°	3.01 kpc
J1840-0809	30.28°	1.02°	6.97 kpc
J1840-0815	34.56°	3.34°	5.04 kpc
J1840-0840	29.08°	0.58°	8.58 kpc
J1840-1122	35.43°	3.85°	4.33 kpc
J1840-1207	28.35°	0.17°	3.71 kpc
J1828-2119	31.25°	4.36°	1.04 kpc
J1829+0000	24.81°	1.07°	10.4 kpc
J1829-0734	23.27°	0.3°	5.20 kpc
J1829-1011	23.11°	0.26°	0.81 kpc
J1829-1751	21.59°	−0.6°	4.69 kpc
J1848-0511	32.76°	0.09°	5.63 kpc
J1848-0601	32.41°	0.07°	6.71 kpc
J1848+0604	33.25°	0.35°	4.05 kpc
J1848+0647	32.37°	−0.04°	6.5 kpc
J1848+0826	34.02°	0.96°	3.39 kpc
J1843-0050	29.57°	0.12°	6.03 kpc

Table 3 continued

Table 3 (*continued*)

Pulsar Name	θ	ϕ	L_i
J1843-0137	29.52°	0.07°	5.70 kpc
J1843-0211	29.4°	0.24°	5.26 kpc
J1843-0355	29.34°	0.04°	5.97 kpc
J1843-0408	28.79°	-0.19°	5.45 kpc

NOTE—List of randomly distributed pulsars averaged for an hypothetical source. The galactic longitude is denoted by θ and the galactic latitude by ϕ . More information about the pulsars can be found [here](#).

In order to better understand the importance of the maximal angle α_m , we will analyze the dependency on the original angular frequency of the incoming gravitational wave, namely Ω , e.g. see eq. (56).

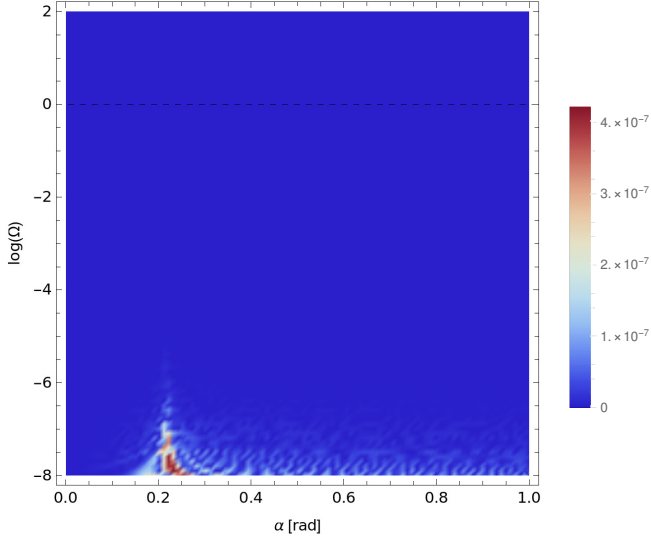


Figure 6. Density plot of $|\tau_{\text{GW}}|$ in terms of the common logarithm of angular frequency Ω and the angle α . This graphic shows why PTAs are so important to measure this effect. Other values given by Tab. 1, with $H_0 = 70$ km/s/Mpc.

From the Figure 6 we can note that for the region with 10^{-6} rad/s $< \Omega < 10^2$ rad/s, the value of $|\tau_{\text{GW}}|$ is practically zero. However, in the region 10^{-8} rad/s $< \Omega < 10^{-6}$ rad/s the

value starts to rise. This is the reason why the other type of detectors as LISA or LIGO are useless in this framework: Only PTA works in the proper range of the frequency spectrum (Barke et al. 2015).

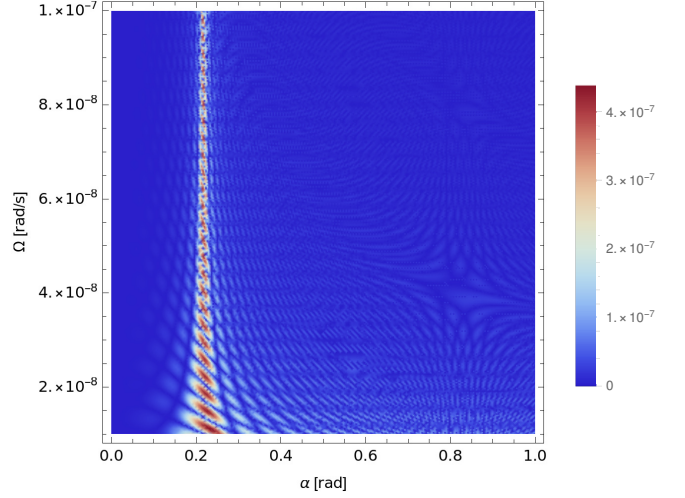


Figure 7. Same plot as Fig. 6 but in the range 10^{-8} rad/s $< \Omega < 10^{-7}$ rad/s. We can note the lack of dependence on Ω .

If we zoom up the Figure 6, i.e. Fig. 7, we can clearly note that for different values of the angular frequency Ω , the maximum value of τ_{GW} corresponds always to the same angle, so Ω has no dynamical consequences in the phenomenon. A similar analysis of L is shown in Fig. 8.

We can note that, once again, no dependency on L is present in Fig. 8. That means no matter what is the distance between the pulsar and the Earth, the maximum value of τ_{GW} will appear always approximately at the same characteristic angle α_m . What about Z ?

From the Figure 9 is clear that for different values of the distance between the Earth and the source of GWs, the angle where the maximum value of τ_{GW} is reached changes dramatically. Therefore, the angle α_m depends on the distance Z in an explicit but unknown way. Finally, let us analyze the case of the Hubble constant.

We can see how the dependency on H_0 in Fig. 10 is quite similar to the dependency on Z in

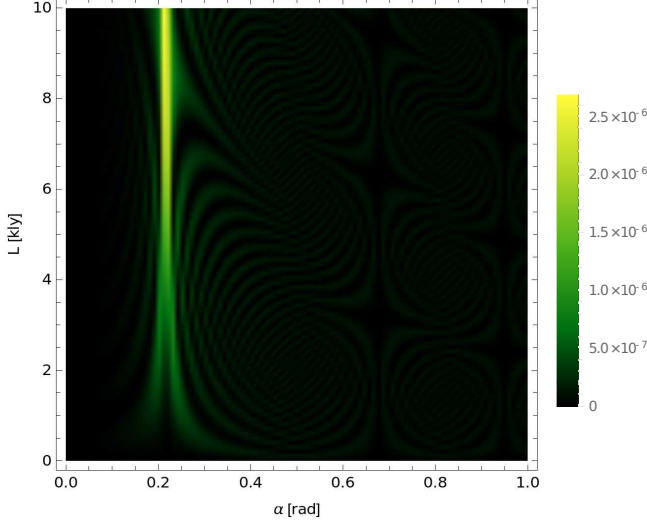


Figure 8. Density plot of $|\tau_{\text{GW}}|$ in terms of the distance L (in light-years), and the angle α . The rest of parameters are given by Tab. 1, with $H_0 = 70$ km/s/Mpc. Again, there is almost no dependence on L .

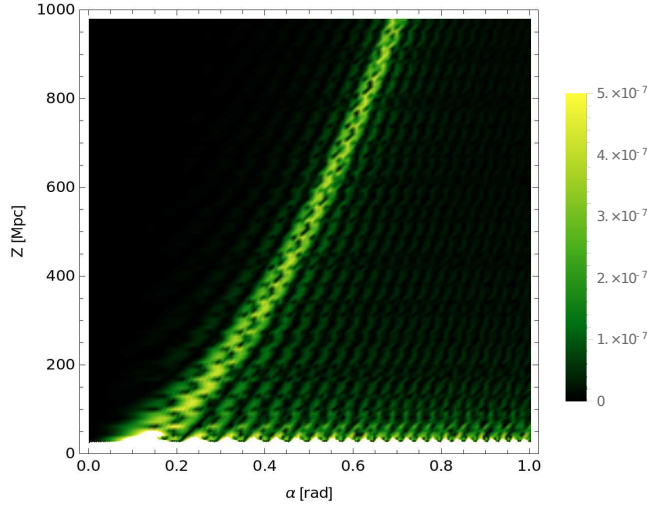


Figure 9. Density plot of $|\tau_{\text{GW}}|$ in terms of the distance Z (in megaparsecs), and the angle α . The rest of parameters are given by Tab. 1, with $H_0 = 70$ km/s/Mpc. Unlike the previous cases, we do see a dependency on Z .

Fig. 9, which gives us a clue about a possible relationship between these parameters. Let us zoom up the Figure 11.

As we can see, the maximum value of the timing residual τ_{GW} (i.e. the white spots) has a

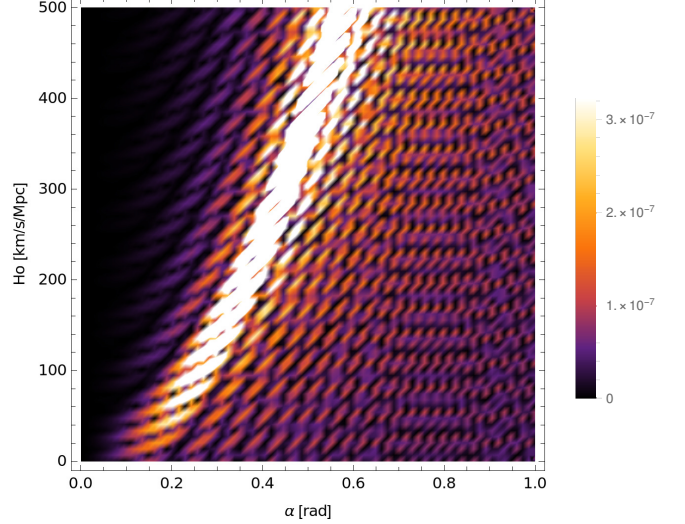


Figure 10. Density plot of $|\tau_{\text{GW}}|$ in terms of the Hubble constant H_0 (in km/s/Mpc), and the angle α . The rest of parameters are given by Tab. 1.

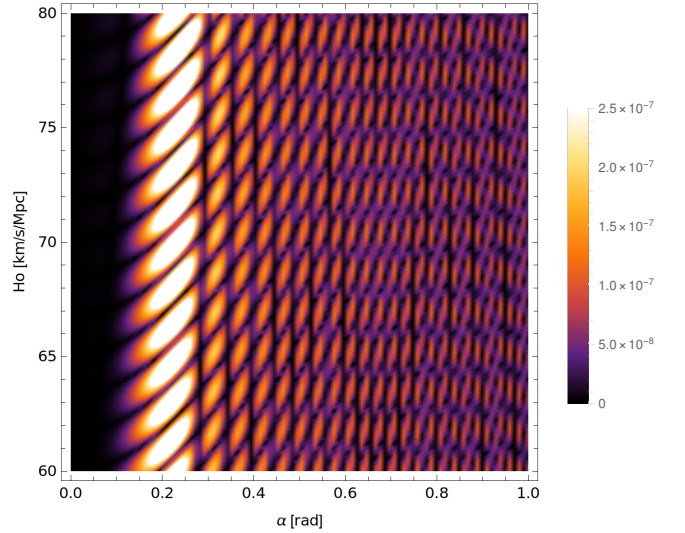


Figure 11. Same plot as Fig. 10 but in the suitable range $60 \text{ km/s/Mpc} < H_0 < 80 \text{ km/s/Mpc}$. We can note a slight slope in angular position, in accordance with Fig. 3.

slightly oscillatory structure around a characteristic maximal angle α_m . It can be noticed that the full white strip has a very small slope, showing a slow variation of the angular position, being in agreement with the Figure 3.

We can summarize the previous analysis as follows: The numerical integration of the equation (55), with the parameters given by the Ta-

ble 1, gives us the density plots shown above. From the Figure 6 we can establish the crucial role of Pulsar Timing Arrays in the eventual measurement of the influence of the cosmological components of the Universe on the propagation of gravitational waves. Furthermore, the Figures 9 and 10 show us that there is a implicit relationship between the values of the Hubble constant, H_0 , the distance between the Earth and the source of Gravitational Waves, Z , and the maximal angle where τ_{GW} reaches its maximum, α_m .

In the next subsection we will look in more detail at the characteristics that τ_{GW} has and, by means of some very reasonable approximations, we will be able to find an analytical expression where the three previously mentioned observables will be present, establishing in this way a possibility to measure the local value of the Hubble constant using the quantities α_m and Z .

3.3. A relationship between PTA observables and the Hubble constant

From the dependencies shown in Fig. 9 and Fig. 10, we can speculate about the existence of a relationship between the value of H_0 and the maximal angle α_m . In order to simplify the computation, we can omit the geometrical prefactor that appears in (55), because it is common to every observation and is H_0 -independent. Therefore, we define a reduced timing residual,

$$\begin{aligned} \tau_{\text{GW}}^{\text{red}} &\equiv \int_{-1}^0 \frac{1 + H_0 [T_e + \frac{xL}{c}]}{Z_e + xL \cos \alpha} \sin\left(\frac{\pi}{4} + \Theta(x, \alpha)\right) dx \\ &\approx R_1 + \left(\frac{1 + \frac{H_0 Z_e}{c}}{Z_e}\right) \int_{-1}^0 \sin\left(\frac{\pi}{4} + \Theta(x, \alpha)\right) dx, \end{aligned} \quad (60)$$

with $|R_1| \leq \frac{LH_0}{cZ_e} \sim 10^{-31}$ s. Neglecting R_1 and maximizing the value of $|\tau_{\text{GW}}^{\text{red}}|$ as a function of α , we obtain

$$H_0 \cong \frac{2c}{Z} \sin^2\left(\frac{\alpha_m}{2}\right). \quad (61)$$

For an in-depth analysis and step-by-step derivation of this formula, see appendix A. The expression in (61) provides a precise relationship between H_0 and the observables α_m and Z . This formula can be used to take an independent and local measurement of the Hubble constant. On the other hand, we know that for a small redshift, i.e. $z \ll 1$, it holds that $z \approx \frac{Z_e}{c} H_0$ (see Ryden 2003) and also equation (51). Thus, when comparing with the equation (61) we also obtain an expression that could be interpreted as the redshift of the source of Gravitational Waves in terms of the maximal angle α_m , given by

$$z \cong 2 \sin^2\left(\frac{\alpha_m}{2}\right) \quad z \ll 1. \quad (62)$$

Notice that (62) provides an independent measurement of the redshift of the source of GW, that could be specially useful if the source is a dark object. In the Figure 12 we show the behavior of the approximation formula with respect to the numerical analysis, included the values and bar errors of current observations.

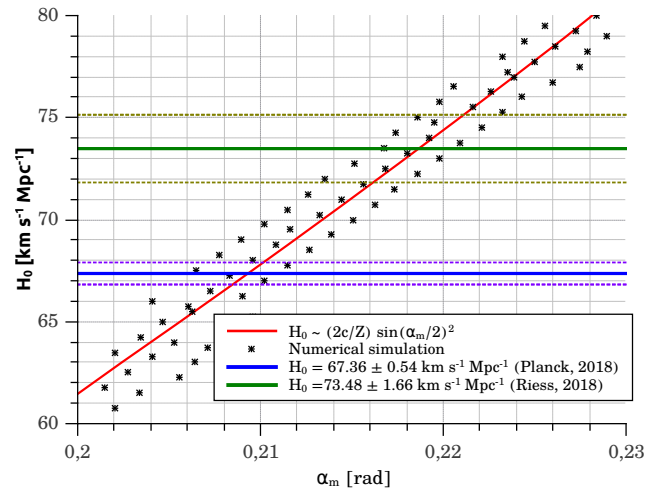


Figure 12. A comparison the value of H_0 with respect to the formula (61) and the numerical maximum of $|\tau_{\text{GW}}|$. The average error in the approximation is of the 1.5% from numerical simulation.

4. CONCLUSIONS

In this paper we have extended the line of research developed in [Bernabeu et al. \(2011\)](#); [Espriu & Puigdomènech \(2013\)](#); [Espriu \(2014\)](#); [Alfaro et al. \(2019\)](#) on the action of cosmological parameters into the propagation of gravitational waves. This effect, an additional contribution besides the redshift in the frequency, is completely due to the coordinates transformation between the GW-centered-frame and the comoving frame where gravitational waves are measured. The main result of this effect is that harmonic gravitational waves measured near the source are actually anharmonic when cosmological observer measure them, i.e. the Earth or PTAs.

In particular, we have extended the previous attempts to a case where all the cosmological contributions (e.g. Dark Energy in form of Λ , non-relativistic matter and radiation) are naturally included inside the Hubble constant. We have shown that all the coordinates transformations involved are linear in terms of H_0 and generalized the theoretical results obtained previously in [Bernabeu et al. \(2011\)](#); [Espriu & Puigdomènech \(2013\)](#); [Espriu \(2014\)](#); [Alfaro et al. \(2019\)](#). We deeply studied the dependencies of the equation (55) in terms of the angular frequency of the GW, Ω , the distance between the Earth and the pulsar, L , the distance between the Earth and the source of gravitational waves, Z , and the Hubble constant itself. From this analysis, we conjectured a relationship between H_0 , α_m and Z , which we finally obtained as the analytical formula (61), showing an unexplored possibility of study the local behavior of H_0 using the data that PTA experiments could provide us.

This local cosmological action appears to be very sensitive to PTA observations (basically due to the frequency spectrum of Gravitational Waves that PTAs could see), reason of why we claim this effect as an independent way of lo-

cally measure the Hubble constant. Although the precise measurement of this influence can be quite complex due to its intrinsic delicacy, some very privileged millisecond pulsars can be measured with incredible accuracy to test gravitational theories ([Manchester 2017](#)) and they also could be useful in order to test this model in the near future. For this reason we believe it is worthwhile to perform a more detailed study of this phenomenon, for example, considering different sources or not monochromatic gravitational waves, in order to have an astrophysically more realistic analysis.

The authors thank D. Espriu and L. Gabbanelli for many interesting conversations. M. Gamonal and J. Alfaro are partially supported by Fondecyt 1150390 and CONICYT-PIA-ACT14177.

APPENDIX

A. ON THE ACCURACY OF THE APPROXIMATION OF H_0

Here we are going to discuss all the steps that lead to the equation (61). In first place, we take the reduced timing residual from (60) and note that R_1 is given by

$$R_1 = \int_{-1}^0 dx \sin \left(\Theta(x, \alpha) + \frac{\pi}{4} \right) \left[\frac{1 + H_0 \left[\frac{Z_e}{c} + \frac{L}{c} x \right]}{Z_e + xL \cos \alpha} - \frac{1 + H_0 \frac{Z_e}{c}}{Z_e} \right]. \quad (\text{A1})$$

Thus we can bound the value of R_1 by

$$\begin{aligned} |R_1| &\leq \frac{L}{Z_e} \int_{-1}^0 \left| \sin \left(\Theta(x, \alpha) + \frac{\pi}{4} \right) \right| \\ &\quad \times \left| \frac{H_0 \left[\frac{1}{c} x \right] - x \frac{L}{Z_e^2} \cos \alpha - x \frac{L}{Z_e} \cos \alpha H_0 \frac{1}{c}}{\left(1 + x \frac{L}{Z_e} \cos \alpha \right)} \right| dx \\ &\leq \begin{cases} \frac{L \left(H_0 \frac{1}{c} + \frac{L}{Z_e^2} |\cos \alpha| + \frac{L}{Z_e} |\cos \alpha| H_0 \frac{1}{c} \right)}{2Z_e \left(1 - \frac{L}{Z_e} \cos \alpha \right)} & \cos \alpha > 0 \\ \frac{L}{2Z_e} \left(H_0 \frac{1}{c} + \frac{L}{Z_e^2} |\cos \alpha| + \frac{L}{Z_e} |\cos \alpha| H_0 \frac{1}{c} \right) & \cos \alpha < 0 \end{cases} \\ &\leq \frac{LH_0}{2Z_e c} + \mathcal{O} \left(\frac{L^2}{Z^3} \right) \sim 10^{-31} \text{ s}. \end{aligned} \quad (\text{A2})$$

Then we can reasonable neglect R_1 in the equation (60). Now we can express $\tau_{\text{GW}}^{\text{red}}$ in terms of the imaginary part of the complex exponential and write, since $\Theta(x, \alpha)$ is quadratic in x :

$$\begin{aligned} \tau_{\text{GW}}^{\text{red}} &= \text{Im} \left\{ \int_{-1}^0 dx e^{i(\Theta(x, \alpha) + \frac{\pi}{4})} \right\} \\ &= \text{Im} \left\{ e^{i(\Theta(x^*, \alpha) + \frac{\pi}{4})} \int_{-1}^0 dx e^{i\lambda(x-x^*)^2} \right\} \\ &= \text{Im} \left\{ B(\alpha) e^{i(\Theta(x^*, \alpha) + \frac{\pi}{4})} \right\}, \end{aligned} \quad (\text{A3})$$

where $B(\alpha)$ is defined as

$$B(\alpha) \equiv \int_{-1}^0 dx e^{i\lambda(x-x^*)^2}, \quad (\text{A4})$$

x^* satisfies $\partial\Theta(x, \alpha)/\partial x \big|_{x=x^*} = 0$,

$$x^* = \frac{-c + c \cos \alpha + Z_e H_0}{(\cos \alpha^2 - 2 \cos \alpha) H_0 L}, \quad (\text{A5})$$

and λ is given by

$$\lambda = \frac{1}{2} \frac{\partial^2 \Theta(x, \alpha)}{\partial x^2} = \frac{1}{2} \frac{\Omega H_0 L^2}{c^2} (\cos \alpha^2 - 2 \cos \alpha). \quad (\text{A6})$$

The integral $B(\alpha)$ can be written in terms of the error function, giving

$$B(\alpha) = \frac{\sqrt{2\pi}}{4}(1+i)\frac{1}{\sqrt{\lambda}} \left[-\operatorname{erf}\left(\frac{\sqrt{2}}{2}(1-i)u^*\right) + \operatorname{erf}\left(\frac{\sqrt{2}}{2}(1-i)(\sqrt{\lambda}+u^*)\right) \right], \quad (\text{A7})$$

where $u^* \equiv \sqrt{\lambda}x^*$. Using the asymptotic expansion of the error functions for $u^* \gg 1$ (see Abramowitz & Stegun 1972), we can write

$$B(\alpha) \approx e^{-z_1^2} \left(1 + \frac{1}{2z_1} \right) \quad z_1 \equiv \frac{\sqrt{2}}{2}(1-i)u^*. \quad (\text{A8})$$

Inserting the last expression into (A3), $\tau_{\text{GW}}^{\text{red}}$ becomes

$$\tau_{\text{GW}}^{\text{red}} \approx \sin\left(C + \frac{\pi}{4}\right) + \frac{1}{2|u^*|} \sin C, \quad (\text{A9})$$

where $C = H_0 Z^2 \Omega / 2c^2$. From this expression we can see that the maximum of $\tau_{\text{GW}}^{\text{red}}$ clearly happens for $u^* \rightarrow 0$. This condition implies, from (A6), that the angle corresponding to the maximum absolute value of τ_{GW} satisfies $x^* = 0$, or, rearranging the terms, the approximation formula (61).

In order to justify the validity of the asymptotic expansion, we can explore around $u^* = 0$, finding that for a variation in the angle $\Delta\alpha$, then $u^* \sim i\sqrt{\frac{Z\Omega}{c}}\Delta\alpha \sim 10^4\Delta\alpha$. Thus, the expansion is well defined for $\Delta\alpha \gg 10^{-4}$.

REFERENCES

- Abbott, B. P., Abbott, R., Abbott, T. D., et al. 2016, *PhRvL*, 116, 061102, doi: [10.1103/PhysRevLett.116.061102](https://doi.org/10.1103/PhysRevLett.116.061102)
- Abramowitz, M., & Stegun, I. 1972, *Handbook of mathematical functions with formulas, graphs, and mathematical tables* (Dept. of Commerce, National Bureau of Standards.)
- Alfaro, J., Espriu, D., & Gabbanelli, L. 2019, *Classical and Quantum Gravity*, 36, 025006, doi: [10.1088/1361-6382/aaf675](https://doi.org/10.1088/1361-6382/aaf675)
- Arzoumanian, Z., Baker, P. T., Brazier, A., et al. 2018, *ApJ*, 859, 47, doi: [10.3847/1538-4357/aabd3b](https://doi.org/10.3847/1538-4357/aabd3b)
- Babak, S., Petiteau, A., Sesana, A., et al. 2016, *MNRAS*, 455, 1665, doi: [10.1093/mnras/stv2092](https://doi.org/10.1093/mnras/stv2092)
- Barke, S., Wang, Y., Esteban Delgado, J. J., et al. 2015, *Classical and Quantum Gravity*, 32, 095004, doi: [10.1088/0264-9381/32/9/095004](https://doi.org/10.1088/0264-9381/32/9/095004)
- Bernabeu, J., Espriu, D., & Puigdomènech, D. 2011, *PhRvD*, 84, 063523, doi: [10.1103/PhysRevD.84.063523](https://doi.org/10.1103/PhysRevD.84.063523)
- Bringmann, T., Kahlhoefer, F., Schmidt-Hoberg, K., & Walia, P. 2018, *PhRvD*, 98, 023543, doi: [10.1103/PhysRevD.98.023543](https://doi.org/10.1103/PhysRevD.98.023543)
- Bull, P., Akrami, Y., Adamek, J., et al. 2016, *Physics of the Dark Universe*, 12, 56, doi: [10.1016/j.dark.2016.02.001](https://doi.org/10.1016/j.dark.2016.02.001)
- Camarena, D., & Marra, V. 2018, *PhRvD*, 98, 023537, doi: [10.1103/PhysRevD.98.023537](https://doi.org/10.1103/PhysRevD.98.023537)
- Cervantes-Cota, J. L., & Smoot, G. 2011, in *American Institute of Physics Conference Series*, Vol. 1396, American Institute of Physics Conference Series, ed. L. A. Ureña-López, H. Aurelio Morales-Técutl, R. Linares-Romero, E. Santos-Rodríguez, & S. Estrada-Jiménez, 28–52
- Cheng, T. P. 2010, *Relativity, Gravitation and Cosmology, a basic introduction* (Oxford University Press)
- Deng, X., & Finn, L. S. 2011, *MNRAS*, 414, 50, doi: [10.1111/j.1365-2966.2010.17913.x](https://doi.org/10.1111/j.1365-2966.2010.17913.x)

- Di Valentino, E., Linder, E. V., & Melchiorri, A. r. 2018, *PhRvD*, 97, 043528, doi: [10.1103/PhysRevD.97.043528](https://doi.org/10.1103/PhysRevD.97.043528)
- Einstein, A. 1916, *Annalen Phys.*, 49, 769, doi: [10.1002/andp.200590044](https://doi.org/10.1002/andp.200590044), [10.1002/andp.19163540702](https://doi.org/10.1002/andp.19163540702)
- Einstein, A. 1918, *Sitzungsberichte der Königlich Preußischen Akademie der Wissenschaften* (Berlin), Seite 154-167.
- Espriu, D. 2014, in *American Institute of Physics Conference Series*, Vol. 1606, American Institute of Physics Conference Series, 86–98
- Espriu, D., & Puigdomènech, D. 2013, *ApJ*, 764, 163, doi: [10.1088/0004-637X/764/2/163](https://doi.org/10.1088/0004-637X/764/2/163)
- Feeney, S. M., Peiris, H. V., Williamson, A. R., et al. 2019, *Phys. Rev. Lett.*, 122, 061105, doi: [10.1103/PhysRevLett.122.061105](https://doi.org/10.1103/PhysRevLett.122.061105)
- Finn, L. S. 2009, *PhRvD*, 79, 022002, doi: [10.1103/PhysRevD.79.022002](https://doi.org/10.1103/PhysRevD.79.022002)
- Freedman, W. L. 2017, *Nature Astronomy*, 1, 0169, doi: [10.1038/s41550-017-0169](https://doi.org/10.1038/s41550-017-0169)
- Hobbs, G., & Dai, S. 2017, *Natl. Sci. Rev.*, 4, 707, doi: [10.1093/nsr/nwx126](https://doi.org/10.1093/nsr/nwx126)
- Hobbs, G., Archibald, A., Arzoumanian, Z., et al. 2010, *Classical and Quantum Gravity*, 27, 084013, doi: [10.1088/0264-9381/27/8/084013](https://doi.org/10.1088/0264-9381/27/8/084013)
- Ko, P., & Tang, Y. 2016, *Physics Letters B*, 762, 462, doi: [10.1016/j.physletb.2016.10.001](https://doi.org/10.1016/j.physletb.2016.10.001)
- LIGO Collaboration, Abbott, B. P., et al. 2017, *Nature*, 551, 85, doi: [10.1038/nature24471](https://doi.org/10.1038/nature24471)
- Manchester, R. N. 2017, *Journal of Astrophysics and Astronomy*, 38, 42, doi: [10.1007/s12036-017-9469-2](https://doi.org/10.1007/s12036-017-9469-2)
- Manchester, R. N., Hobbs, G. B., Teoh, A., & Hobbs, M. 2005, *AJ*, 129, 1993, doi: [10.1086/428488](https://doi.org/10.1086/428488)
- Mörtsell, E., & Dhawan, S. 2018, *Journal of Cosmology and Astro-Particle Physics*, 2018, 025, doi: [10.1088/1475-7516/2018/09/025](https://doi.org/10.1088/1475-7516/2018/09/025)
- Odderskov, I., Hannestad, S., & Haugbølle, T. 2014, *Journal of Cosmology and Astro-Particle Physics*, 2014, 028, doi: [10.1088/1475-7516/2014/10/028](https://doi.org/10.1088/1475-7516/2014/10/028)
- Perlmutter, S., Gabi, S., Goldhaber, G., et al. 1997, *ApJ*, 483, 565, doi: [10.1086/304265](https://doi.org/10.1086/304265)
- Planck Collaboration, Aghanim, N., Akrami, Y., et al. 2018, *arXiv e-prints*, arXiv:1807.06209. <https://arxiv.org/abs/1807.06209>
- Riess, A. G., Filippenko, A. V., Challis, P., et al. 1998, *AJ*, 116, 1009, doi: [10.1086/300499](https://doi.org/10.1086/300499)
- Riess, A. G., Casertano, S., Yuan, W., et al. 2018, *ApJ*, 861, 126, doi: [10.3847/1538-4357/aac82e](https://doi.org/10.3847/1538-4357/aac82e)
- Ryden, B. 2003, *Introduction to Cosmology* (San Francisco: Addison-Wesley)
- Verbiest, J. P. W., Lentati, L., Hobbs, G., et al. 2016, *MNRAS*, 458, 1267, doi: [10.1093/mnras/stw347](https://doi.org/10.1093/mnras/stw347)